

Time-frequency analysis of single-point engine-block vibration measurements for multiple excitation-event identification

S. Vulli^a, J.F. Dunne^{a,*}, R. Potenza^a, D. Richardson^b, P. King^b

^a*Department of Engineering and Design, The University of Sussex, Falmer, Brighton BN1 9QT, UK*

^b*Advanced Powertrain Engineering, Jaguar Cars Limited, Engineering Centre, Abbey Road, Whitley, Coventry CV3 4LF, UK*

Received 18 July 2007; received in revised form 29 July 2008; accepted 8 October 2008

Handling Editor: C.L. Morfey

Available online 28 November 2008

Abstract

The short-term-Fourier-transform (STFT) is used to identify different sources of IC engine-block vibration from single-point acceleration measurements taken with a commercial knock sensor. Interest is focused on using the STFT to distinguish normal combustion from other sources of excitation including valve impact, injector pulses, and abnormal combustion, such as knocking. Positive identification of these other events using a single method can be useful for pre-processing of measured knock-sensor data for neural-network-based reconstruction of cylinder pressure. It can also be useful separately as part of a fast knock detection system. A series of experiments is discussed to create the data to isolate these different events on a 3-cylinder gasoline engine. In each case, the measured data is processed using the STFT to attempt to isolate the occurrence of particular events in the time domain. Four classes of experiments are undertaken: (i) an un-fired (motored) engine, driven by a dynamometer, with spark plugs fitted, and then removed, to isolate valve impact; (ii) a fired engine running under idle conditions, to contrast no-load combustion with no combustion; (iii) a part-loaded engine running normally, and then running with one injector switched-off, and (iv) a fully-loaded engine running normally, and then running with knock-control switched-off. The paper shows that a single Time-frequency analysis method, applied to knock sensor data in the form of an appropriately-tuned STFT, can effectively identify the occurrence of these events in the time domain if responses are adequately separated and strong enough.

© 2008 Elsevier Ltd. All rights reserved.

1. Introduction

Vibration measurements taken with a knock sensor, fitted to the head or block of an IC engine, are used within knock control strategies [1–5]. Knock sensors are robust, durable, and inexpensive accelerometers capable of measuring high-bandwidth signals from which changes in high frequency content can be used to detect abnormal combustion associated with engine knocking. Vibration measurements are also useful for cylinder pressure reconstruction [6–13], as an indirect way of avoiding the cost and durability issues associated with direct pressure measurement using sensors. This is achieved by feeding single-point vibration measurements into an appropriate inverse vibration model, which in principle can enable gas pressure traces

*Corresponding author.

E-mail address: j.f.dunne@sussex.ac.uk (J.F. Dunne).

to be reconstructed. Accurate cylinder pressure reconstructed in real time, can in turn be used within engine feedback-control strategies for improving thermodynamic efficiency and reducing CO₂ emissions, as well as managing or reducing harmful tailpipe and noise emissions.

A particular problem for both vibration-based cylinder pressure reconstruction [11] and knock detection (assuming that for cylinder pressure reconstruction, an inverse vibration model actually exists) is that with single-point measurements multiple excitation sources [11] can undermine the ability to reconstruct or detect, as appropriate. These additional excitation sources include piston-slap, bearing-impact, gear-meshing, valve impact, and fuel-injector-pulses [14–18]. In the case of cylinder pressure reconstruction, the difficulty with additional sources is they produce responses different from the effect of normal gas pressure. Under normal running conditions, these additional responses actually dominate. At higher speeds however, the occurrence of destructive knock-induced vibration may dominate [13]. Unless the responses associated with these additional events are excluded from the measured histories, the ability of an inverse vibration model to accurately reconstruct cylinder pressure will be seriously undermined. For knock detection, the problem is that the occurrence of these additional events may create high frequency responses that can be misinterpreted by a knock-detection algorithm as engine knock. This paper focuses on a single fast method of identifying the responses to these events.

Several general observations can be made about these additional excitation sources. For example, they tend to be cyclo-stationary [9], but with uncertainty associated with cycle-to-cycle variability [11]. In addition, there may be near-chaotic nonlinear interactions, such as can arise from piston motion [15]. Most of these cyclic events last for a very short duration, and since modal-damping levels are relatively high, responses decay quickly. If the response signature for one of these additional events could be identified, then assuming no overlap or noise corruption, an appropriate time-window could be used to exclude a rapidly-decaying single-point response measurement. Indeed a model-based approach, essentially exploiting knowledge of the system to construct a signature, could be used to synthesise the response to a known pulse arising at an injector, or valve seat. The signature could then be identified using for example a matched filter or correlation detector. There are however four reasons in practise [13] why this is difficult: (i) a huge level of refinement would be needed in the physical model (for example using finite element analysis) such that the model would need to be massive; (ii) it is impossible to predict meaningful high frequency responses associated with a particular signature using a nominal model (regardless of how well refined it is) owing to the effects of small variations in geometry, material properties, and manufacture on a real engine-block; (iii) pulse-loading associated with many of these additional events are themselves variable and subject to some uncertainty; and (iv) the existence of a large number of secondary sources of excitation effectively embeds the particular signature in a background of noise. In view of these physical difficulties with model-based prediction, blind identification using signal processing tools offers a greater prospect of success.

The ideal requirement then for blind identification of additional event responses is a single robust method fast enough for real-time implementation. The method should accurately identify the start and finish of these partially overlapping events buried in noise (and should also be capable of identifying isolated knocking since this too is a source of corruption in cylinder pressure reconstruction). The desire is to exclude responses to these events using the shortest time-window possible. Direct use of the FFT, or more appropriately FFT-based power spectral density estimation, is indeed fast, and offers appropriate noise filtering capabilities, but it is not suitable for identifying non-stationary overlapping events with rapid changes in both time and frequency content. Continuous engine knock can be detected using the FFT but prompt initial knock detection requires use of Time-frequency information [5]. In general time-frequency analysis is commonly approached using the short-term Fourier transform (STFT) or wavelet transform (WT) [19]. Time-Frequency analysis has been used in many automotive applications including for noise studies in powertrain systems [20], combustion analysis [2–5,21–23], and multiple-event identification [24]. The higher resolution capabilities of an appropriate WT, should in principle make it a most effective method for additional event identification since it generally has good time resolution at high frequency. But selection of an optimum wavelet does in fact depend on the characteristics of the signal being detected, which is difficult to generalise, potentially sensitive to background noise, and therefore unlikely to be possible with a single approach. By contrast the STFT is easier to use, less sensitive to window type, with relatively few commonly-used window types to choose from. But the STFT has not been widely applied to additional event identification because of its known poor time resolution

capabilities at high frequency. For practical use of time-frequency analysis however, whichever approach is adopted, appropriate engine data needs to be generated that will allow the effectiveness of the analysis to be established. In this paper a series of experiments are described to generate precisely the required data to allow the effectiveness of the STFT to be established for additional event identification. Emphasis focuses on the use of a single, suitably-tuned STFT, to establish whether this one method is appropriate for identifying: (i) valve events; (ii) injector pulses; and (iii) engine knock.

2. Time-frequency analysis using the STFT

Time-frequency analysis can be approached using a variety of transforms including the (windowed) or STFT, the wavelet, the chirplet, the fractional Fourier, and the Newland transforms. The problem with the Fourier transform in general, is its inability to simultaneously resolve in the time, and frequency domains. There is a necessary trade-off in so-called window selection, between good time, and good frequency resolution. If the chosen window has very good time resolution, then this will be achieved at the expense of poor frequency resolution. The STFT (which although computationally very fast) does not completely solve the time-frequency dilemma. This may explain why there has been a reluctance to use the STFT for combined mechanical-event and knock detection. This paper examines whether this reservation is justified. First the STFT will be briefly defined, then applied in tuned form.

The continuous STFT $F(t, \omega)$ of a continuous-time function $f(t)$ is defined as:

$$F(\tau, \omega) = \int_{-\infty}^{+\infty} f(t)w(t - \tau)e^{-j\omega t} dt \quad (1)$$

where the window function $w(t)$ generally satisfies the condition:

$$\int_{-\infty}^{+\infty} w(\tau) d\tau = 1 \quad (2)$$

The spectrogram function $S(t, \omega)$ is defined as:

$$S(\tau, \omega) = |F(\tau, \omega)|^2 \quad (3)$$

In discrete time, the STFT becomes:

$$F(m, \omega) = \sum_{n=-\infty}^{\infty} f[n]w[n - m]e^{-j\omega n} \quad (4)$$

where the discrete time window function $w[n]$ satisfies a discrete-time version of Eq. (2). There is also a discrete-time version of the spectrogram function defined by Eq. (3). The effect of the short-duration window function $w(n)$ is to slide along the signal length, to enable construction of the Fourier transform of the product $f(t)w(t-\tau)$ at each value of discrete time m , allowing the local frequency content to be estimated. To apply the STFT selectively to measured engine-block vibrations, an appropriate series of engine experiments are needed, as now explained.

3. Engine test programme and experimental data acquisition

A 3-cylinder in-line SI engine was used to generate the test data. This directly-injected 4-stroke gasoline engine was fitted with fixed valve timing, EGR, and full knock control. The engine was coupled to a DC dynamometer and fitted with spark-plug-mounted piezo-electric pressure sensors on all cylinders (Kistler type 6117B). The engine has a firing order 1-3-2. Engine block vibrations were measured with a knock sensor (Bosch type A-261-231-114), of identical type to the existing sensor fitted for knock control. Data acquisition was achieved using an MTS RedLine-ACAP System, along with combustion parameter monitoring using ETK-ES690 hardware, interfaced with INCA-software. The engine has a compression ratio = 11.5:1; a displacement = 1125 cm³; and a maximum torque = 98 Nm at 3750 rev/min. The (Bosch) fuel injector-spray cone-angle = 70°; the minimum fuel injection pulse-width = 0.1 ms; the con rod length = 137 mm, and the pin

offset = 0.8 mm. As far as the fixed valve timing was concerned, the details are as follows: IVO = 6° BTDC, IVC = 42° ABDC, EVO = 40° BBDC, EVC = 4° ATDC, and the valve overlap-angle = 10°.

3.1. Experimental test programme

Four classes of experiment were undertaken: (i) an un-fired motored engine, driven by a dynamometer, with spark plugs fitted, and then removed, to isolate valve impact; (ii) a fired engine, running under idle conditions, to contrast no-load combustion with no combustion; (iii) a part-loaded engine running normally, and then running with one injector switched-off, and (iv) a fully-loaded engine running normally, and then running with knock-control switched-off. The purpose of these tests is now explained.

- (i) Dynamometer-driven (motored) engine at 1000 rev/min with spark-plugs removed and re-fitted: The purpose of this test with spark-plugs removed was to create no-compression, to generate response data corresponding to moving parts and valve-motion impact forces only. With the spark-plugs replaced, the motored engine responses correspond to mechanical noise plus combustion-free cylinder pressure.
- (ii) Fired-engine running under idle conditions at 1000 rev/min: this test was to generate data to enable a contrast be made between responses with no combustion in (i), as compared with responses for no-load combustion. This data also contains responses to injector-pulses.
- (iii) Part-loaded engine running normally at 1000 rev/min and load torque of 28 Nm, then running at the same speed and load with one injector switched-off: In this test, the fuel injector in cylinder-2 was switched-off. The purpose in this highly-unbalanced running condition, was to create data both with, and without injector-pulse-induced responses and corresponding combustion events. For this reason the test was conducted only for a short duration. The engine was run at a speed of 1000 rev/min and measurements taken of: (a) pressure in cylinder-1, (b) the separately-fitted knock sensor response, and (c) the TDC-locator signal for cylinder-1.
- (iv) Fully-loaded engine running normally, then running with knock-control switched-off: The purpose of this test was to create normal-condition fully-loaded (no-knock) response data, and corresponding response data for a knocking condition. To induce engine knocking, the output from the knock control sensor was deliberately disconnected.

3.2. Data acquisition

Two different sampling methods were available using the RedLine-ACAP data acquisition system, namely: (1) crank-angle-based sampling, and (2) time-based sampling. Crank-based sampling is generally the most suitable for sampling engine test data. Sampled-time intervals are not in general constant since discrete samples are taken in response to pulses delivered by a digital shaft-encoder fitted to the engine crankshaft. This allows data to be samples at specified fractions of a revolution depending on the number of pulses-per-revolution (ppr) of the encoder. Most combustion events occur at different angular positions of the crankshaft and therefore can easily be located with crank-based sampling. However control over the sampling frequency is not possible—this is determined by the engine-crank speed and by the ppr of the encoder. Crank-based data sampling is therefore not readily suitable for identifying fixed-step discrete-time mathematical models. Moreover even ignoring the fact that real-time stepping is variable, the sampling frequency is usually too low for vibration analysis. For example when the engine runs at 1000 rev/min with a 360 ppr encoder, the sampling-rate would be around 6 KHz. This data cannot therefore be analysed using STFT technique (or used for training a neural network model for pressure reconstruction via engine-block vibrations).

Temporal sampling by contrast, involves fixed-time-step sampling controlled as usual by an internal clock, such that the sampling rate is independent of the crank speed. The disadvantage with this method is that combustion events cannot be readily referenced to crank position, therefore the number of data samples varies from one cycle to another cycle owing to slight fluctuations in engine speed. This loss of reference position can be partly overcome by using additional information, such as piston-TDC location signals, spark-plug, and injector control pulses. The major advantage of temporal sampling is that the data is readily suitable for

identifying discrete-time mathematical models. For vibration analysis involving combustion events, high sampling-rates are needed for capturing acceleration data. This is because activities such as valve-impact and injector-pulse forcing are high-frequency events (generating responses up to 20 kHz). For these reasons, constant time-sampling was used instead of crank-based-sampling. An additional sensor was located on the flywheel-end of the engine to locate the TDC position of cylinder-1. This sensor was useful to locate the start-point and end-point of a cycle. Most of the energy in acceleration signals was spread between 10–15 KHz, and in the measured pressure signals, in the range 1.5–2 KHz. In all of these experiments, time-based sampling frequency was fixed at a rate of 100 kHz (all measured cylinder-pressure signals were also appropriately ‘pegged’ [13]).

4. Measured engine-block vibration analysis using the STFT

Initially a study was undertaken to find a single set of parameters and an appropriate window function $w[n]$ to provide an optimum compromise between time and frequency resolution using the STFT (Eq. (4)) for all the test cases (i)–(iv) in Section 3.1. Appropriate tuning suggested use of a Gaussian window function, with a single set of optimum parameters, namely 512-data point sections, and an overlapping length of 498-points. The results of the STFT analysis are now explained.

4.1. Results for motored engine at 1000 rev/min with spark-plugs removed and then re-fitted

Figs. 1a–d shows results for the ‘no-compression’ test. Valve opening and closing events can be identified from the TDC-locator signal (and from the valve-time diagrams not shown). Fig. 1a for example, shows one-cycle of measured knock sensor acceleration including the TDC-locator pulse for cylinder-1. This can be used to locate where the peak pressure would be under normal operation, also allowing the relative location of additional events to be established. Application of the STFT Eq. (4) to the measured knock sensor acceleration, followed by computation of the spectrogram function via Eq. (3), is shown first in 2D in Fig. 1b, and in a 3D-view in Fig. 1c. A discrete Fourier transform (DFT) of the entire acceleration signal is shown in Fig. 1d. Figs. 2a–d show results for the data obtained from the motoring test at 1000 rev/min with the spark plugs re-fitted to examine mechanically-induced vibrations, particularly caused by valve motion activity. Fig. 2a shows one-cycle of measured knock sensor acceleration, and the measured cylinder pressure for cylinder-1. Application of the STFT (Eqs. (4) and (2)) to the raw acceleration is shown in 2D in Fig. 2b, and in 3D in Fig. 2c. A DFT of the entire acceleration signal is shown in Fig. 2d.

4.1.1. Discussion of results for spark-plugs removed and then re-fitted

Without compression, the responses shown in Fig. 1a (over two revolutions) are mainly caused by valve activity. An interval of around 240° (or 0.04s) occurs between these events. Fig. 1a shows that transient responses have totally decayed before a combustion event (identified by the cylinder-1 TDC-locator). The interval between these responses depends on the relative proximity of the valve-pulse to the knock sensor, but a detailed examination of the valve-timing information given in Section 3, shows the dominant excitation source is exhaust-valve closure (EVC). EVC for a different cylinder, occurs 22° after inlet-valve closure (IVC) or 0.0036s later. The spectrogram in Fig. 1b shows occurrences of EVC as broad-band responses but resolution of the lower-intensity IVC response (shortly before) is however not possible. When compression is restored (by replacing the spark plugs) the dominant response is still caused by combined IVC and EVC. Between these events, Fig. 2b and c show localised lower-intensity broad band responses caused by motorised cylinder pressure. A possible source here is pressure-induced bearing impact. Figs. 1d and 2d show, as expected, that direct application of a DFT to acceleration data, cannot locate events in time. The STFT clearly enables these responses to be excluded from the acceleration measurements.

4.2. Results for engine idling at 1000 rev/min

Figs. 3a–d show results obtained from measured data for the engine running at 1000 rev/min in an idle condition. Fig. 3a shows one-cycle of measured knock sensor acceleration and the measured cylinder pressure

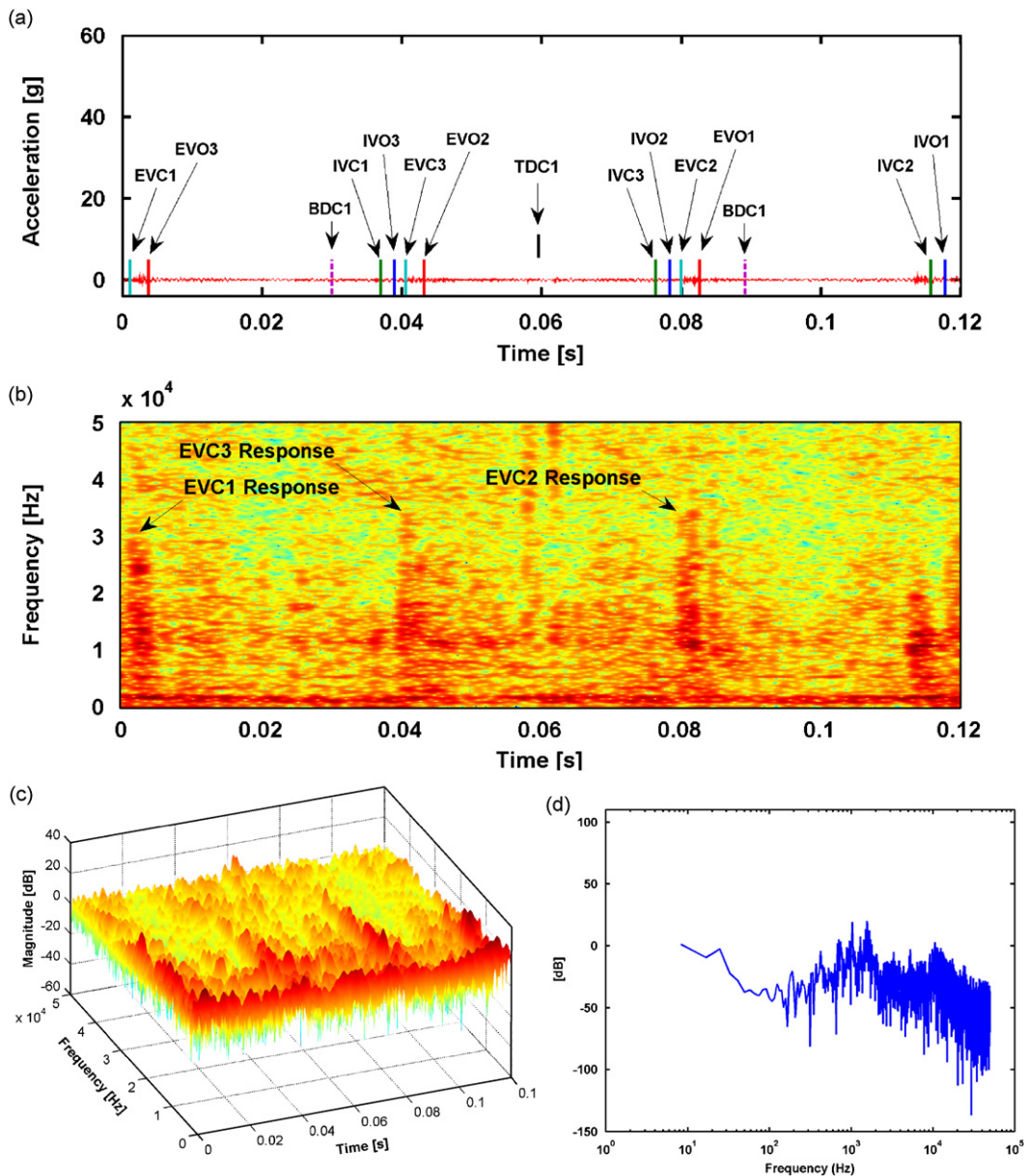


Fig. 1. Engine motoring without compression at 1000 rev/min (with all spark-plugs removed): (a) acceleration via knock sensor, showing all valve events, TDC and BDC for cylinder-1; (b) time-frequency analysis of one-cycle of knock sensor acceleration; (c) time-frequency surface for one-cycle of knock sensor acceleration; (d) discrete Fourier transform of knock sensor acceleration.

for cylinder-1. Application of the STFT Eqs. (4) and (2) to the raw acceleration is shown in 2D in Fig. 3b, and in 3D in Fig. 3c. A DFT of the entire acceleration signal is shown in Fig. 3d.

4.2.1. Discussion of results for engine idling at 1000 rev/min

In the previous two test cases, valve impact-induced vibration and general mechanical vibration sources were examined. When the engine fires normally, there are two more excitation sources—one due to injector pulses, the other a response to combustion gas-pressure forces. The total duration of injector activity in this test, was between 2 and 5 ms as shown in Fig. 3a. The phase difference for injectors in different cylinders is

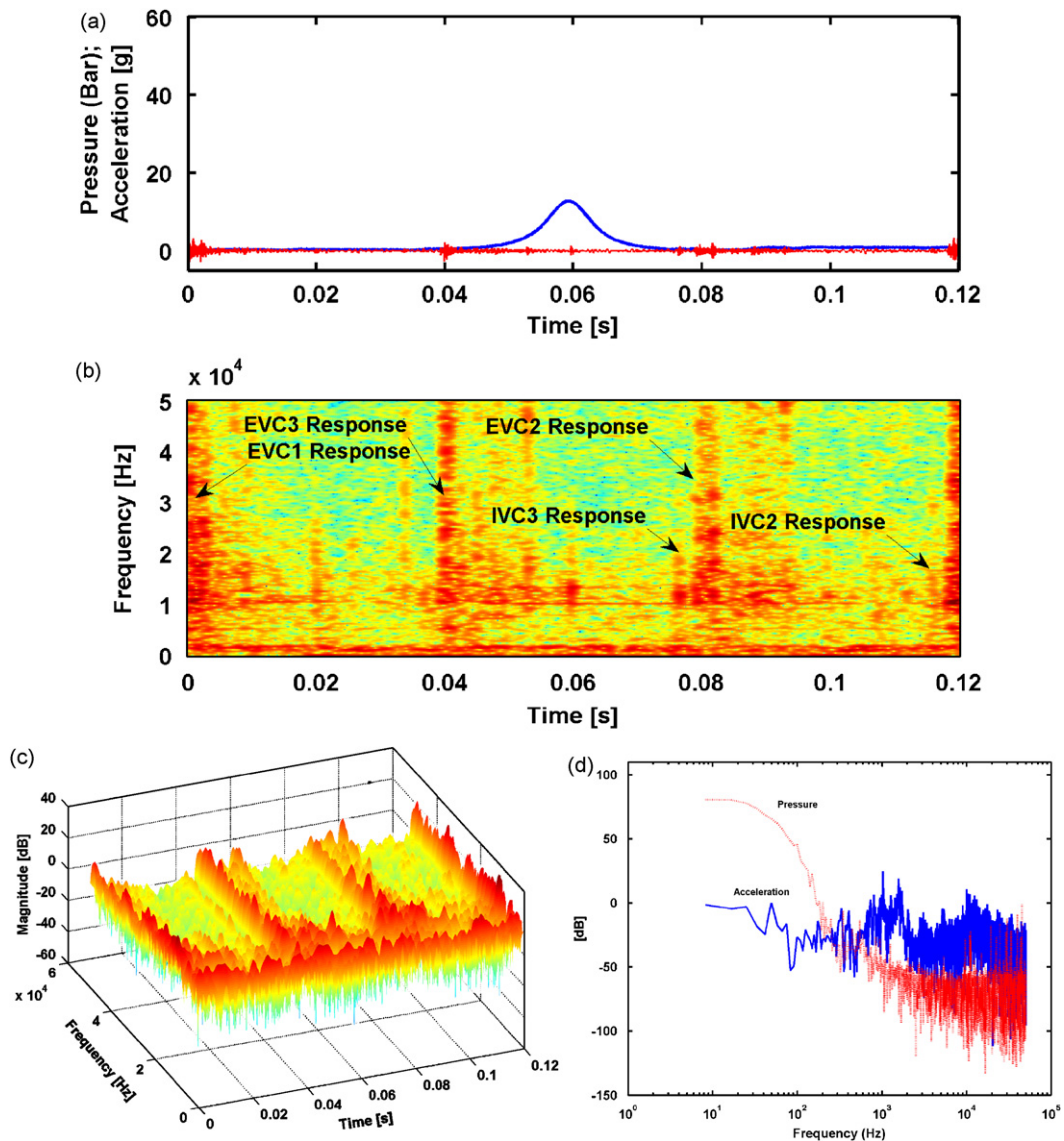


Fig. 2. Engine motoring at 1000 rev/min: (a) cylinder pressure and knock sensor measurements; (b) time-frequency analysis of one-cycle of knock sensor acceleration; (c) time-frequency surface for one-cycle of knock sensor acceleration; (d) discrete Fourier transform of knock sensor acceleration.

240° CA, or 0.04s duration. Comparison of the pressure-acceleration histories in Fig. 2a, for the motoring condition, confirms that valve-impact overlaps injector-pulses. The effect of injector-pulses dominate over the other effects, with large accelerations magnitudes (around 60 g maximum). Note that the small spike at TDC in Fig. 2a has vanished at TDC in Fig. 3a. This is the much-reduced effect of piston ‘tipping over’ under idle condition owing to the piston being controlled by increased cylinder pressure from combustion as opposed to just motoring. Analysis of the measured pressure from cylinder-1 using a DFT in Fig. 3d, shows the combustion pressure trace has a maximum energy concentrated in the combustion zone (0.058–0.068 s), with magnitudes as large as 75 dB, spread over a frequency range from 0 to 600 Hz. Comparison of the time-frequency content of the acceleration measurements in Fig. 3b and c, clearly identifies the sources of vibration, since valve-impact is similar to the motoring test. However valve-impact and injector-pulses overlap. Engine-block vibrations caused by injector pulses are very significant in magnitude as shown in Fig. 3b, occurring, respectively, at 0.005, 0.045, and 0.085 s, for cylinders 1, 3, and 2. The injector-pulse

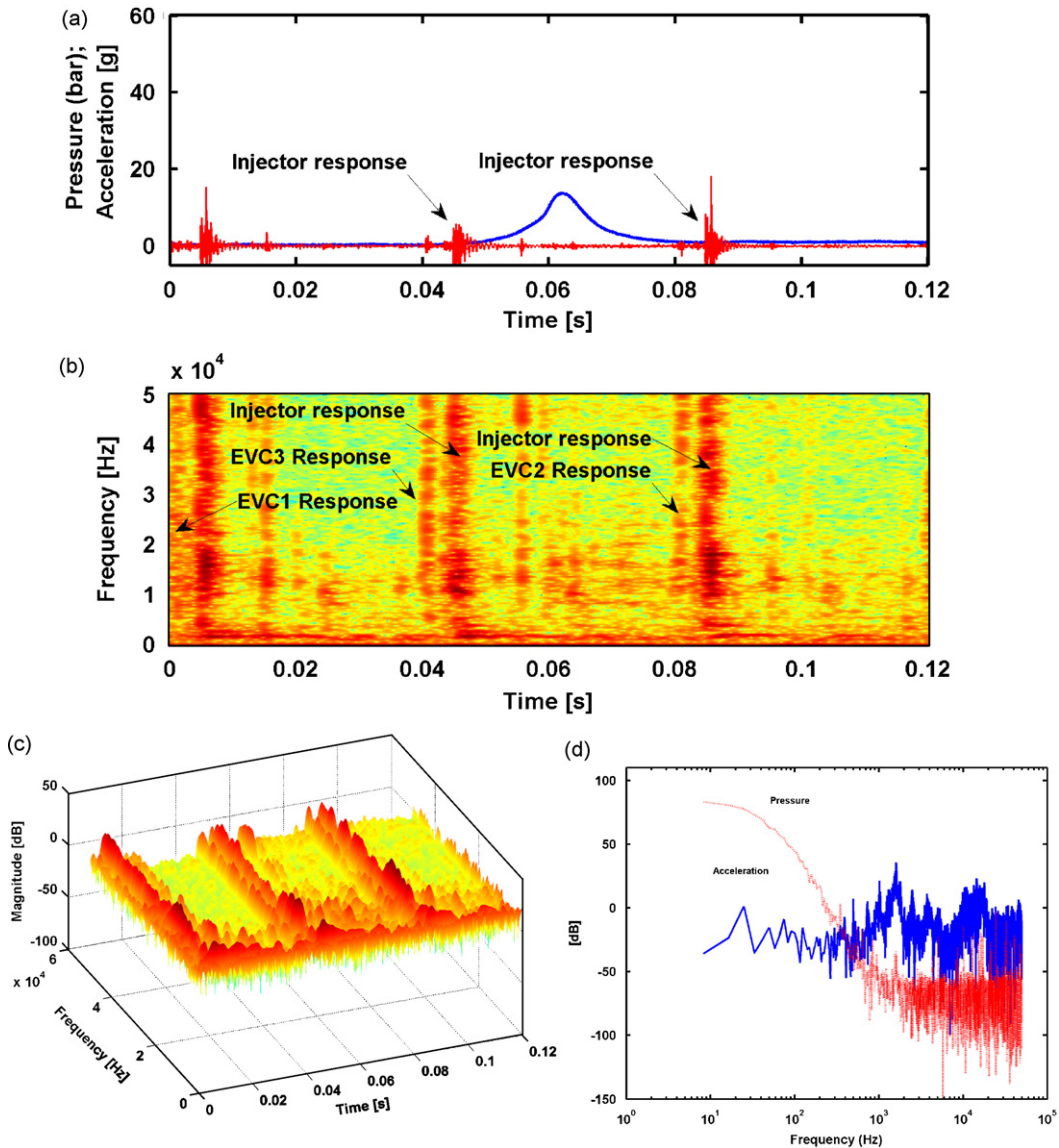


Fig. 3. Engine running under idle condition at 1000 rev/min: (a) pressure and knock sensor measurements; (b) time-frequency analysis of one-cycle of knock sensor acceleration; (c) time-frequency surface for one-cycle of knock sensor acceleration; (d) discrete Fourier transform of cylinder pressure and knock sensor acceleration.

response frequencies span a wide range of frequencies from 0–20 KHz, with large magnitudes of 50–60 dB. Analysis of the combustion-induced vibrations at respective times of 0.025, 0.065, and 0.085 s (for cylinders 1, 3, and 2) showed that the higher energy magnitudes were 30–40 dB, in two ranges of frequencies, from 0 to 2 KHz, and 5–10 KHz. The transient vibrations caused by both valve-impact and injector-pulses have no effect on the combustion-induced vibrations (see Fig. 3c). This test confirms that valve and injector pulse responses can be separated using a data window on the time axis.

4.3. Results for part-loaded engine running normally then with one injector switched-off

Figs. 4a–d, and Figs. 5a–d, show, respectively, the results for two separate test cases both at an engine speed of 1000 rev/min and a load torque of 28 Nm, initially with all the fuel injectors on, and then with one injector

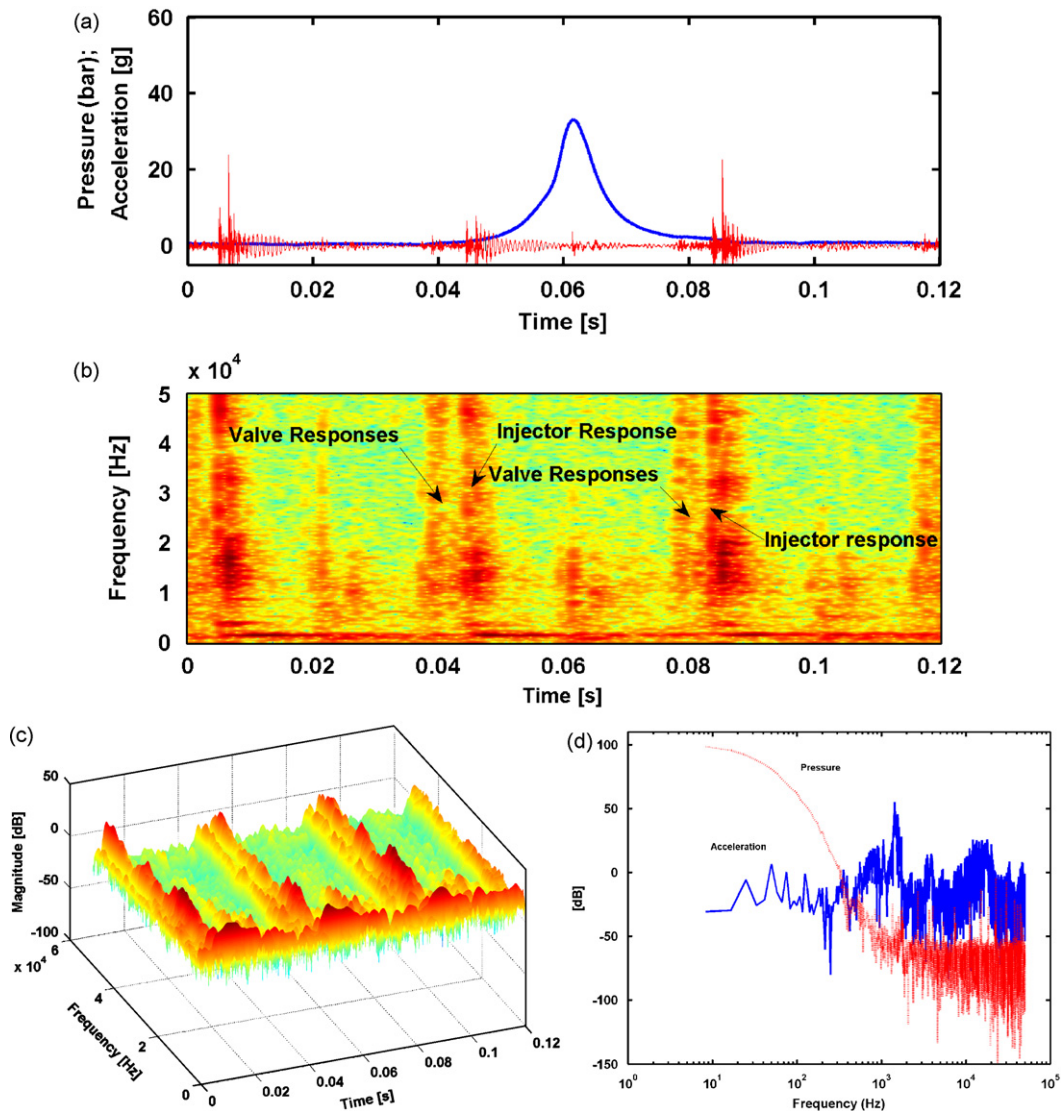


Fig. 4. Engine running normally at 1000 rev/min and 28 Nm: (a) pressure and knock sensor measurements; (b) time-frequency analysis of one-cycle of knock sensor acceleration; (c) time-frequency surface for one-cycle of knock sensor acceleration; (d) discrete Fourier transform of cylinder pressure and knock sensor acceleration.

for cylinder-2, switched off. Fig. 4a shows one-cycle of measured knock sensor acceleration for the ‘all-injectors-on’ case, and the corresponding measured cylinder pressure for cylinder-1. Application of the STFT (Eqs. (4) and (2)) to the raw acceleration is shown in 2D in Fig. 4b, and in 3D in Fig. 4c. A DFT of the entire acceleration signal is shown in Fig. 4d. Fig. 5a by contrast shows one-cycle of measured knock sensor acceleration and the measured cylinder pressure for cylinder-1 for the ‘one-injector-off’ case. Application of the STFT Eq. (4) to the raw acceleration is shown in 2D in Fig. 5b, and in a 3D-view in Fig. 5c. A DFT of the entire acceleration signal is shown in Fig. 5d.

4.3.1. Discussion of results for ‘injector-on’ and ‘injector-off’ cases

Injector-pulse induced vibrations can be more clearly seen in this case in a way that is less possible for the idling test case, as the valve-motion induced vibrations overlapped the injector pulses. The magnitude of the peak-pressure in Fig. 5a is clearly more than the peak-pressure in Fig. 4a. By turning-off the injector for cylinder-2, the corresponding injection-induced vibrations are obviously absent. In particular, note the

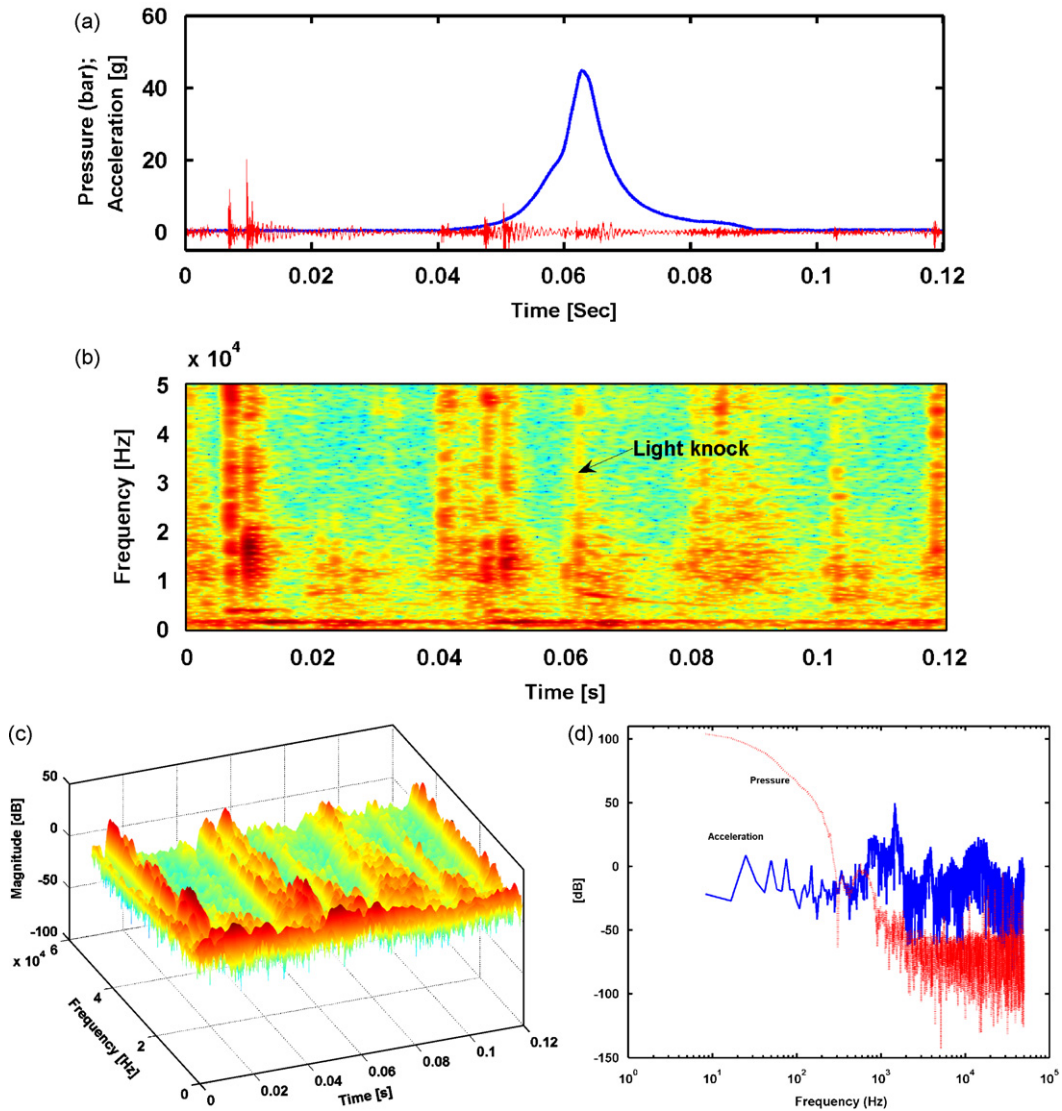


Fig. 5. Engine running at 1000 rev/min and 28 Nm with cylinder-2 injector ‘off’: (a) pressure and knock sensor measurements; (b) time-frequency analysis of one-cycle of knock sensor acceleration; (c) time-frequency surface for one-cycle of knock sensor acceleration; (d) discrete Fourier transform of cylinder pressure and knock sensor acceleration.

differences around the time of 0.08 s on Figs. 4a and 5a, respectively. There is only valve-motion induced vibration present in this zone in the “no-injection” case. When all the injectors are ‘on’, the pressure (with a maximum magnitude of 35 bar) for cylinder-1 has (significant) energy of 70 dB in a frequency range of 0–600 Hz (Fig. 4d). When the cylinder-2 injector was “off”, the magnitude of the peak-pressure (maximum magnitude of 45 bar), and its corresponding energy of 80 dB, were found to be higher. By isolating the injector pulse-induced, and valve-motion-induced vibrations (as in Fig. 5b and c), it is clear that the injector-pulses dominate over valve impact in the total response of the system. Valve-impact has a smaller frequency range i.e. from 0–15 KHz, with relatively small magnitudes. Even in this case, transient vibrations from injector-pulse induced vibrations have no effect on the gas-pressure induced vibrations. It is also worthy of note that with only two injectors active, to maintain the same torque of 28 Nm, cylinder pressures are higher than with three cylinders firing. The shape of the pressure trace with two cylinders firing, suggests that knock control was

active, which is visible from the compression pressure ‘lifting off’. Therefore since light knock was occurring, as expected a vibration response is evident just after peak pressure.

4.4. Results for fully-loaded engine running normally, then with knock-control switched-off

This section shows how the STFT with the same parameters as used previously can also be useful for identifying engine knock. Two sets of data are obtained at an engine speed of 1800 rev/min, and an almost maximum load of 85 Nm. In normal operation of the engine, the knock (control) sensor was connected as normal to the ECU, whereas to generate knock, it was disconnected. Figs. 6a–d and Figs. 7a–d, show the respective sets of results. Fig. 6a shows one-cycle of measured knock sensor acceleration and the measured cylinder pressure for cylinder-1 for the ‘one-injector-off’ case. Application of the STFT Eq. (4) to the

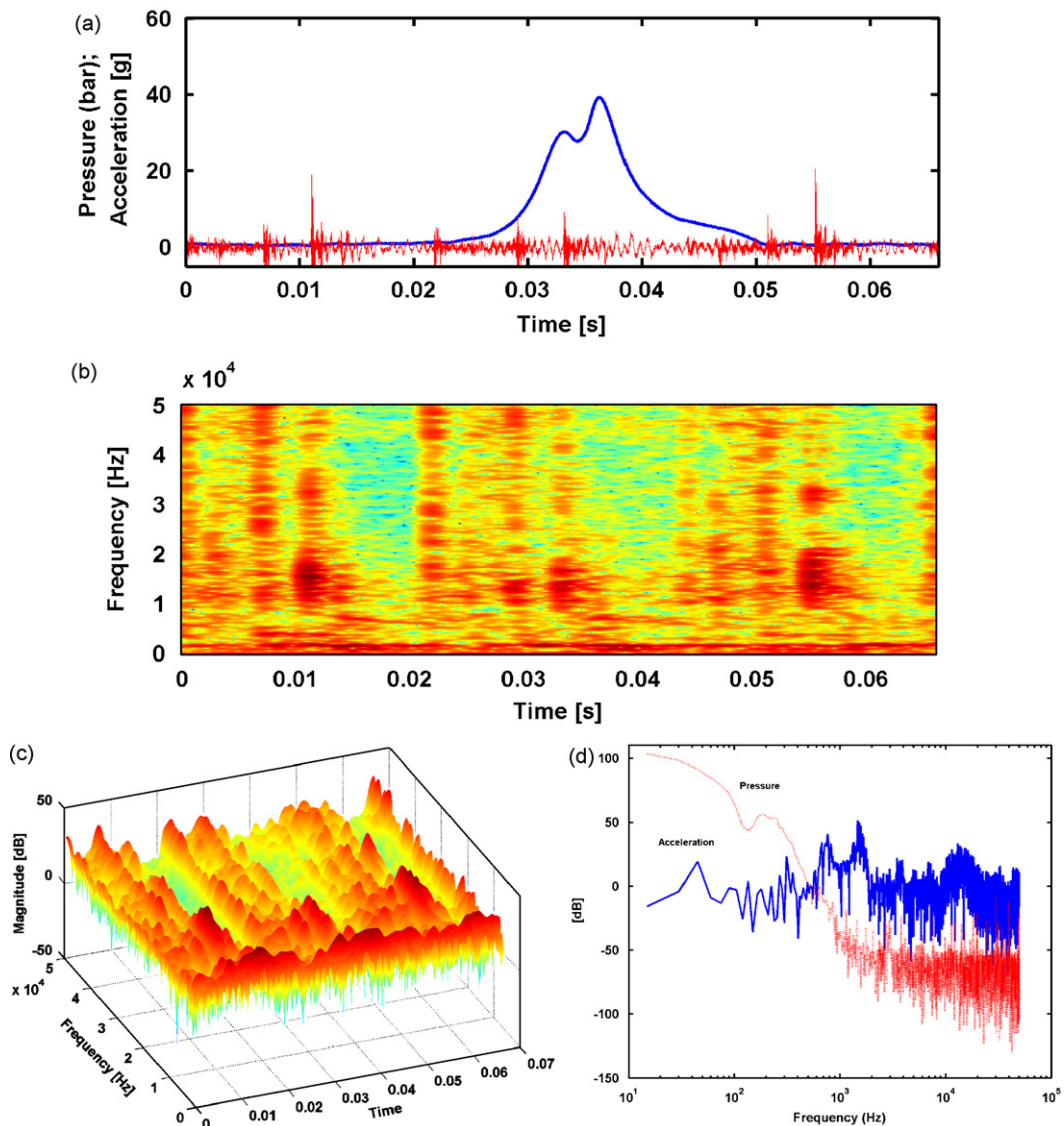


Fig. 6. Engine running normally at 1800 rev/min and 85 Nm: (a) pressure and knock sensor measurements; (b) time-frequency analysis of one-cycle of knock sensor acceleration; (c) time-frequency surface for one-cycle of knock sensor acceleration; (d) discrete Fourier transform of cylinder pressure and knock sensor acceleration; (e) time-frequency analysis of one-cycle of cylinder pressure; (f) time-frequency surface for one-cycle of cylinder pressure.

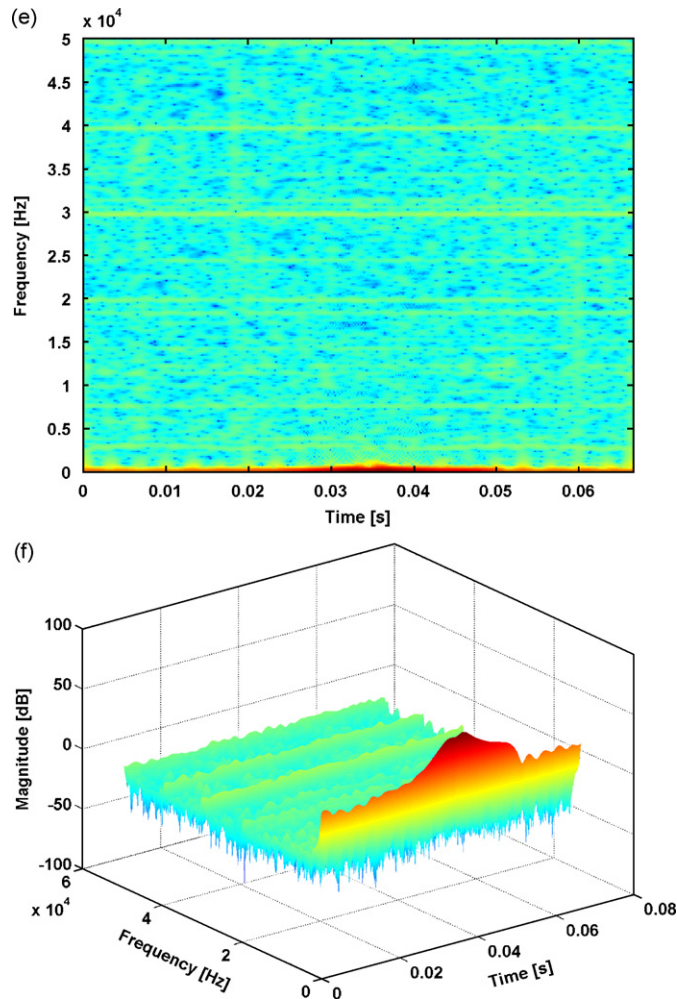


Fig. 6. (Continued)

raw acceleration data is shown in 2D in Fig. 6b, and in 3D in Fig. 6c. A DFT of the entire acceleration signal is shown in Fig. 6d. Figs. 6e and f, respectively, show application of the STFT to the measured cylinder pressure in 2D and 3D. Fig. 7a–f show a corresponding set of results for knock control disconnected.

4.4.1. Discussion of results for fully-loaded engine running normally, then with knock-control switched-off

Particular engine test-points already identified created conditions where knock would be known to occur. Figs. 6a and 7a shows one cycle of pressure and acceleration data for normal and abnormal operations. Figs. 6d and 7d show respective applications of the DFT. It is clearly easier to differentiate normal from abnormal (knocking) conditions if exact cylinder-pressures are known and the DFT is applied. Indeed in the knocking engine, very low amplitude high frequency oscillations are visible in the measured pressure trace. This is also very evident when the STFT is applied to measured pressure data as in Figs. 7e and f in comparison with Figs. 6e and f (where there is no knock). However application of the STFT to acceleration data clearly shows knocking by comparing Figs. 6b and 7b and Figs. 6c and 7c, respectively (around 0.04 s). By contrast direct application of the DFT to acceleration data as compared in Figs. 6d and 7d, respectively, makes knock identification very difficult.

5. Conclusions

The short term Fourier transform has been used to identify different sources of IC engine-block vibration from single-point acceleration measurements taken with a commercial knock sensor. A series of experiments has isolated different events on a 3-cylinder gasoline engine. From the analysis, the following conclusions can be drawn: (i) a suitably-tuned STFT, with a single set of control parameters, when applied to measured acceleration is capable of identifying strong valve impact, injector-pulses and engine knock; (ii) the STFT is unsuitable for separating closely-overlapping or weak events such as the block-responses to inlet valve closure and exhaust valve closure (from a different cylinder). But this is not a problem for time domain exclusion of rapidly-decaying responses for vibration-based neural network reconstruction of cylinder pressure; and

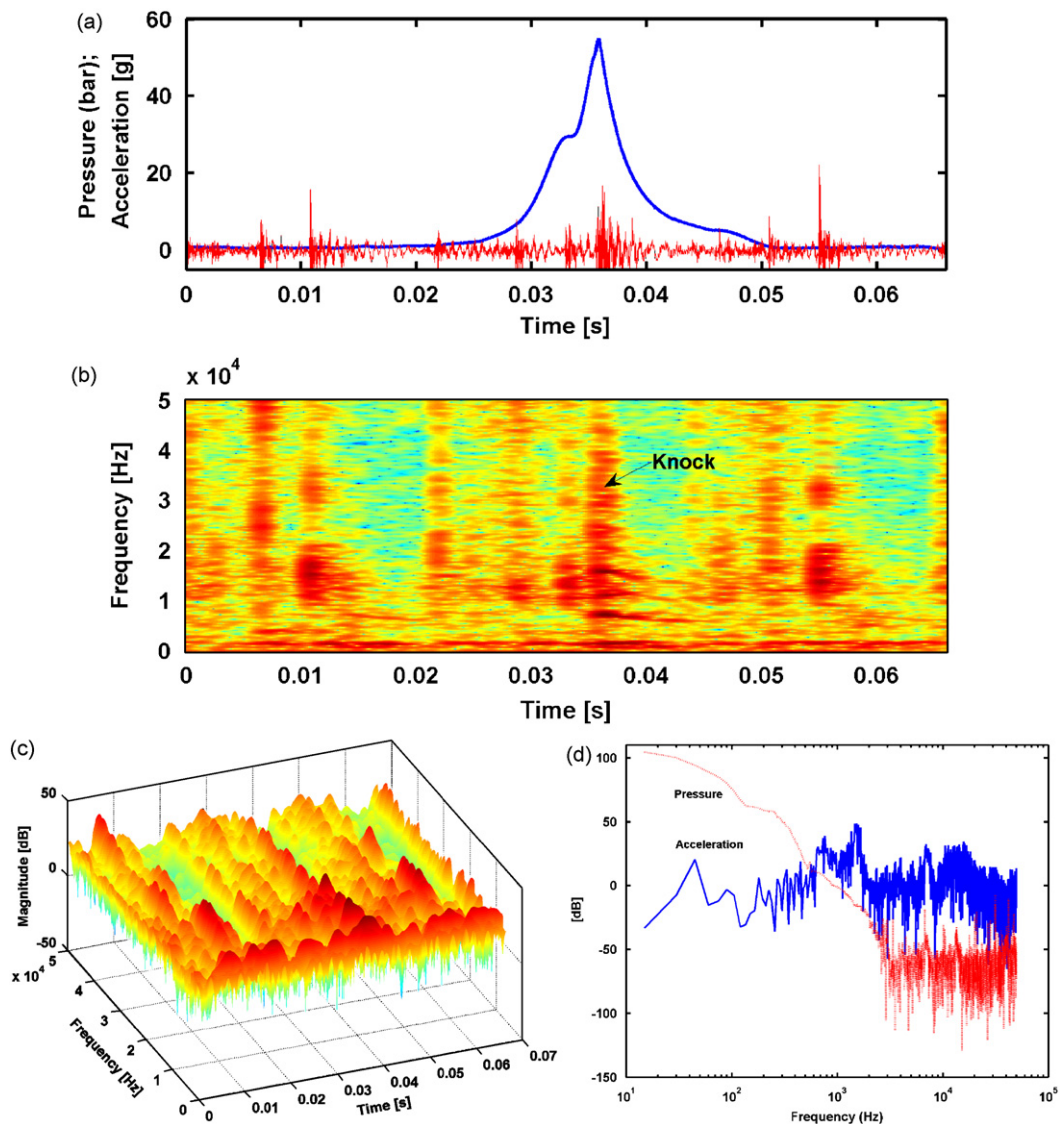


Fig. 7. Engine running under 'knock' conditions at 1800 rev/min and 85 Nm: (a) pressure and knock sensor measurements; (b) time-frequency analysis of one-cycle of knock sensor acceleration; (c) time-frequency surface for one-cycle of knock sensor acceleration; (d) discrete Fourier transform of cylinder pressure and knock sensor acceleration; (e) time-frequency analysis of one-cycle of cylinder pressure; (f) time-frequency surface for one-cycle of cylinder pressure.

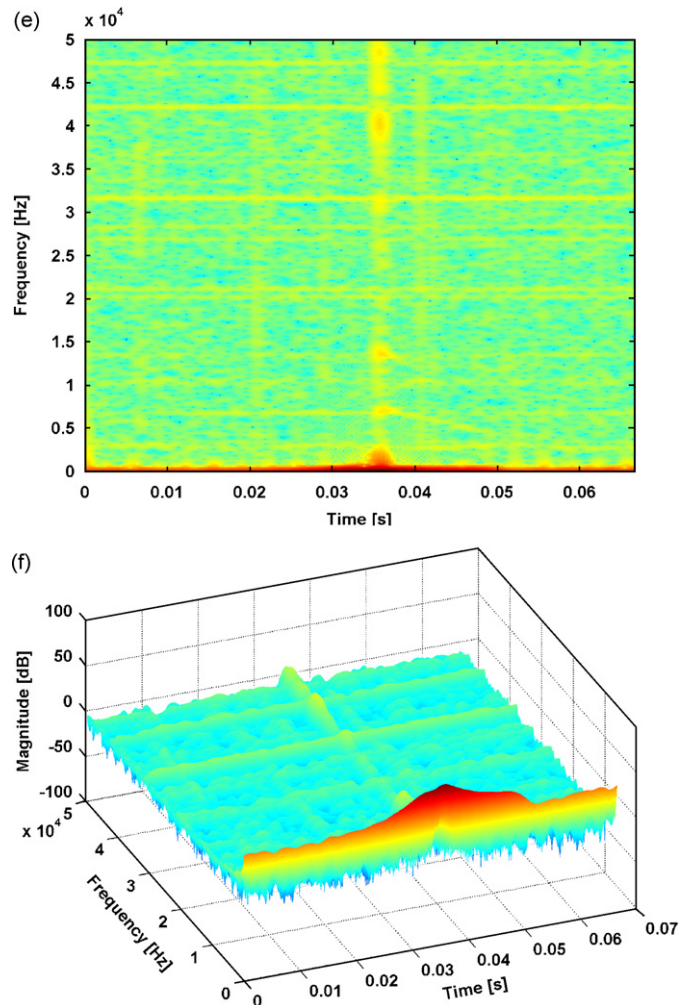


Fig. 7. (Continued)

(iii) direct application of the DFT to pressure data is an easy way to identify knock, but application of the STFT to pressure data is better. The overall conclusion of the paper is that a single time-frequency analysis applied to knock sensor data using an appropriately-tuned STFT, can quite effectively identify the occurrence of these events in the time domain provided responses are adequately separated and strong enough.

Acknowledgements

The authors wish to acknowledge the generous support of Jaguar Cars Ltd. in this project, and for permission to publish the work. The very helpful technical support of the Ford Dunton European Powertrain Research and Development Group is also acknowledged.

References

- [1] J.H. Thomas, B. Dubuisson, M.A. Dillies-Peltier, Engine knock detection from vibration signals using pattern recognition, *Meccanica* 32 (5) (1997) 431–439.
- [2] Z. Zhang, E. Tomota, A new diagnostic method of knocking in a spark-ignition engine using the wavelet transform, 2000, SAE-2000-01-1801.

- [3] J. Chang, M. Kim, K. Min, Detection of misfire and knock in spark ignition engines by wavelet transform of engine block vibration signals, *Measurement Science and Technology* 13 (7) (2002) 1108–1114.
- [4] J. Fu, N. Kurihara, Knock detection for SI engine using wavelet transform (in Japanese), *Transactions of the Japan Society of Mechanical Engineers C* 69 (688) (2003) 3215–3220.
- [5] S. Ker, F. Bonnardot, L. Duval, Algorithm comparison for real time knock detection, *ICASSP 2007 (IEEE International Conference on Acoustics, Speech and Signal Processing, Honolulu)* Vol. 2, 2007, pp. 397–400.
- [6] M. Kao, J.J. Moskwa, Nonlinear diesel engine control and cylinder pressure observation, *Journal of Dynamic Systems, Measurement, and Control* 116 (1995) 183–192.
- [7] Y. Gao, R.B. Randall, Reconstruction of diesel engine cylinder pressure using a time domain smoothing technique, *Mechanical Systems and Signal Processing* 13 (5) (1999) 709–722.
- [8] H. Du, L. Zhang, X. Shi, Reconstructing cylinder pressure from vibration signals based on radial basis function networks, *Proceedings of the Institution of Mechanical Engineers Part D: Journal of Automobile Engineering* 215 (D6) (2001) 761–767.
- [9] J. Antoni, J. Daniere, F. Guillet, R.B. Randall, Effective vibration analysis of IC Engines using cyclostationarity. Part II—New results on the reconstruction of the cylinder pressures, *Journal of Sound and Vibration* 257 (5) (2002) 839–856.
- [10] M. Urlaub, J.F. Böhme, Reconstruction of pressure signals on structure-borne sound for knock investigation, SAE Technical Paper No. 2004-01-0521, 2004.
- [11] R. Johnsson, Cylinder pressure reconstruction based on complex radial basis function networks from vibration and speed signals, *Mechanical Systems and Signal Processing* 20 (8) (2006) 1923–1940.
- [12] S. Vulli, J.F. Dunne, R. Potenza, A recurrent neural network for vibration-based engine cylinder pressure reconstruction, *Ninth International Conference on Recent Advances in Structural Dynamics, ISVR*, 2006.
- [13] S. Vulli, Cylinder Pressure Reconstruction Using Neural Networks and Knock-sensor Measurements, DPhil Dissertation, University of Sussex, 2007.
- [14] R.S. Paranjape, Development of a Math-Based Piston Noise Model, SAE-980564, 1998.
- [15] S. Balakrishnan, H. Rahnejat, Isothermal transient analysis of piston skirt-to-cylinder wall contacts under combined axial, lateral, and tilting motion, *Journal of Physics D: Applied Physics* 38 (2005) 787–799.
- [16] M.H. Chien, Engine impact noise measurement and quantification, SAE-951236, 1995.
- [17] T. Tomoda, M. Kubota, R. Shimizu, Numerical analysis of mixture formation of a direct injection gasoline engine, *The Fifth International Symposium on Diagnostics and Modelling of Combustion in Internal Combustion Engines*, July 1–4, Nagoya, 2001.
- [18] R. Rotondi, G. Bella, Gasoline direct-injection spray simulation, *International Journal of Thermal Sciences* 45 (2006) 168–179.
- [19] L. Cohen, *Time-Frequency Analysis*, Prentice Hall Inc., Englewood Cliffs, NJ, 1996.
- [20] T.N. Patro, Combustion Induced Powertrain NVH—A Time-Frequency Analysis, SAE-971874, 1997.
- [21] F. Molinaro, F. Castanié, A. Denjean, Knocking recognition in engine vibration signal using the wavelet transform, *Proceedings of the IEEE-SP International Symposium*, 4–6 October 1992, pp. 353–356.
- [22] Y. Yajima, K. Nakashima, New measuring technique of cylinder pressure spectrum and its application to combustion noise reduction—time-frequency analysis of combustion excitation using wavelet transformation analysis, *JSAE Review* 19 (1998) 277–282.
- [23] H. Furumaya, J. Suzuki, J. Fu, N. Kurihara, Combustion diagnosis of SI engine using wavelet transform (in Japanese), *Nihon Kikai Gakkai Nenji Taikai Koen Ronbunshu* 5 (2004) 257–258.
- [24] L. Stankovic, J.F. Böhme, Time-frequency analysis of multiple responses in combustion engine signals, *Journal of Signal Processing* 79 (1999) 15–28.